Sensitivity analysis of periprosthetic healing to cell migration, growth factor and post-operative gap using a mechanobiological model

Pascal Swider[a]*, D. Ambard[a], G. Guérin[a], Kjeld Søballe[b] and Joan E. Bechtold[c]

[a]*IMFT UMR CNRS 5502, University of Toulouse, CHU Purpan, Amphithéâtre Laporte, Place Dr Baylac, 31056 Toulouse Cedex, France;* [b]*Department of Orthopaedic Surgery, University of Aarhus, Aarhus Amtsyggehus, Aarhus, Denmark;* [c]*Biomechanics Laboratory, Midwest Orthopaedic Research Foundation and Minneapolis Medical Research Foundation, Minneapolis, MN, USA*

A theoretical rationale, which could help in the investigation of mechanobiological factors affecting periprosthetic tissue healing, is still an open problem. We used a parametric sensitivity analysis to extend a theoretical model based on reactive transport and computational cell biology. The numerical experimentation involved the drill hole, the haptotactic and chemotactic migrations, and the initial concentration of an anabolic growth factor. Output measure was the mineral fraction in tissue surrounding a polymethymethacrylate (PMMA) canine implant (stable loaded implant, non-critical gap). Increasing growth factor concentration increased structural matrix synthesis. A cell adhesion gradient resulted in heterogeneous bone distribution and a growth factor gradient resulted in homogeneous bone distribution in the gap. This could explain the radial variation of bone density from the implant surface to the drill hole, indicating less secure fixation. This study helps to understand the relative importance of various host and clinical factors influencing bone distribution and resulting implant fixation.

Keywords: implant fixation; computational cell biology; mechanobiology; osteoblast; anabolic growth factor; reactive transport in porous media

List of symbols

ϕ_s (%)	structural fraction
C_g (ng/mm^3)	growth factor concentration
α_s (mm^6/cell s ng)	structural fraction synthesis
C_{g0} (ng/mm^3)	initial GF concentration
ρ (kg/mm^3)	density
D_g (mm^2/s)	growth factor diffusion
ϕ_f (%)	fluid fraction or porosity
r_i (mm)	implant radius
q_f (mm/s)	fluid flux
r_d (mm)	drill-hole radius
C_o (cell/mm^3)	cell concentration
r_b (mm)	host bone radius
α_o (m^3/cell s)	cell proliferation
ϕ_{si} (%)	structural fraction at implant
n_o (cell/mm^3)	proliferation threshold
ϕ_{sm} (%)	mean structural fraction
D_o (mm^2/s)	cell random diffusion
$\Delta\phi_s$ (%)	heterogeneity index
χ_o (mm^5/s ng)	chemotactic coefficient
$u, \bar{u}$	output measures
h_o (mm^5/s kg)	haptotactic coefficient
a_i	coefficients of experimental design

1. Introduction

Joint replacement implants with stable and secure mechanical conditions post-operatively are associated with higher longevity (Hahn et al. 1998). In general, low mineralisation of newly formed tissue or bone that is located heterogeneously (i.e. without complete contact between native bone and implant surface) decreases clinical performance (Søballe et al. 1992; Morshed et al. 2007). The characteristics of the bone that forms in the vicinity of the implant are affected by surgical technique, the amount of implant stability gained at surgery and interactions between biochemical factors such as coatings, growth factors and cells in the periprosthetic space (Albrektsson et al. 1983; Wang et al. 1997; Overgaard 2000; Anderson 2001; Colnot et al. 2007; Schwarz et al. 2007).

In periprosthetic healing, predominately intramembranous bone forms without a cartilagenous phase. Osteoblasts are the cells promoting bone formation and mineralisation, and various growth factors can help to promote bone matrix formation (Conover 2000). Osteoclasts and osteoblasts interact, but this is not included here. There are many anabolic growth factors, and the TGF-β superfamily is known to promote bone formation. It has mitogenic action on osteoblasts and can stimulate matrix formation via autocrine, paracrine and endocrine modes (Roberts 2000). Growth factors regulate the cell differentiation, proliferation and motility (Linkhart et al.

*Corresponding author. Email: swider@cict.fr

1996; Kibbin 1998). Osteoblasts are lining cells, which diffuse and actively move along surfaces. Cell migration mechanisms such as haptotactic and chemotactic migrations play a significant role in their dispersal (Lauffenburger et al. 1983; Puleo et al. 1991; Friedl et al. 1998; Dee et al. 1999). Haptotactic migration describes the cell motility by way of adhesion sites and porosity gradients, whereas the chemotactic migration causes cell motions by way of chemical factor gradients.

This type of a system lends itself to numerical modelling, and early attempts focused on the mechanical conditions (Lauffenburger et al. 1983; Dee et al. 1999; Cowin 2001). The addition of biological factors to improve the clinical relevance of these initial mechanical models has recently been undertaken (Ramamurti et al. 1997; Geris et al. 2008; Puthumanapully et al. 2008; Checa and Prendergast 2009). Significant progress has been obtained in predictive modelling but quantitative evaluation against *in vivo* or *ex vivo* data is complex and still rare.

There is a significant level of uncertainty regarding the assignment of parameter values to represent *in vivo* conditions, particularly when biologic and mechanical conditions are combined. This leads to concerns related to the robustness of the model. Accordingly, we implemented a parametric sensitivity analysis to elucidate how clinical, mechanical and biochemical parameters influence predicted periprosthetic tissue distribution. Biological tissue was considered a multiphasic convective-diffusive-reactive medium (Ambard et al. 2005). The predictive model has been evaluated by comparison with histomorphometric data from a stable implant model (Ambard and Swider 2006).

2. Materials and methods

The method was based on our original formulation combining mechanical conditions with computational cell biology (Ambard and Swider 2006). The initial description of the model was followed by the numerical experimentation.

2.1 Governing equations

The tissue volume unit shown in Figure 1 was considered to express the diffusive-convective-reactive Equation (1). The output measure u was the structural fraction or mineralised fraction of newly formed tissue ϕ_s, the interstitial fluid flux q_f, the osteoblast concentration C_o and the anabolic growth factor concentration C_g. Coefficients L, C, D and Ω were detailed in appendix (Equations (A1)–(A4)).

$$L\frac{\partial u}{\partial t} = D\Delta u - C\nabla u + \Omega. \qquad (1)$$

Equation (A1) expresses the balance of the fluid fraction ϕ_f. The volumes of cell and growth factor phases were considered negligible compared to those of the structural and fluid phases. As a consequence, the sum of ϕ_s and ϕ_f was equal to 1.0 and ϕ_f also expressed the porosity of the multiphasic medium.

The osteoblast concentration C_o was described by the conservative Equation (A2) involving random diffusion and active migrations (Maheshwari and Lauffenburger 1998; Fall et al. 2002; Meinel et al. 2003). The gradient of growth factors $\partial C_g/\partial x$ directed the chemotactic flux and the gradient of structural fraction $\partial \phi_s/\partial x$ directed the haptotactic flux. Both influenced the convection and source terms of Equation (A2). The cell source represented the proliferation process using a logistic law where α_o and n_o were the rate of cell divisions and the proliferation threshold, respectively.

The growth factor concentration C_g was described by the conservative Equation (A3). It includes random diffusion and convection which was dependant upon the fluid flux q_f and the porosity gradient $\partial \phi_f/\partial x$. To limit the complexity of the problem, no production or consumption term was considered.

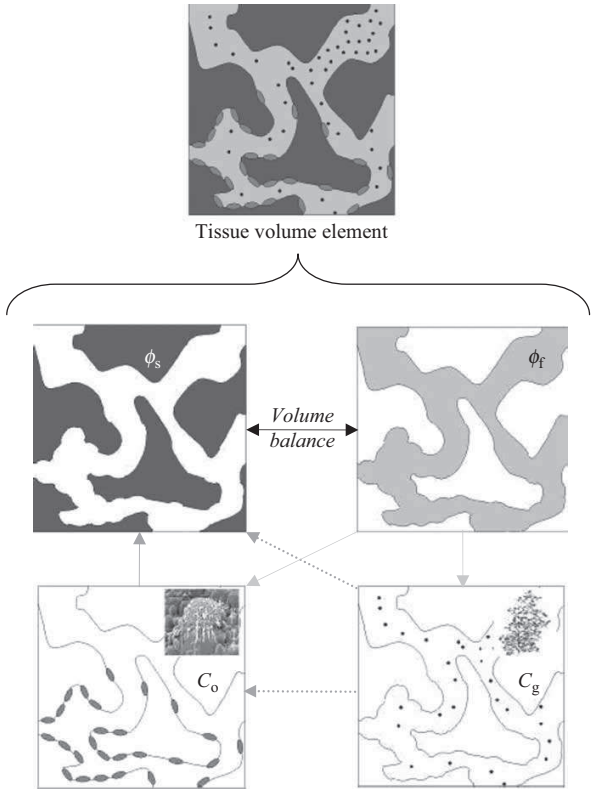

Figure 1. Flow chart showing interactions in the model of tissue healing. Four phases interacted in the diffusive-convective-reactive model whose variables were the structural (or mineralised) fraction ϕ_s, the extracellular fluid phase ϕ_f (or porosity), the osteoblast concentration C_o and the growth factor concentration C_g.

The synthesis of the structural fraction ϕ_s was modelled using the source term in Equation (A4). The synthesis was directed by α_s acting together with the fluid, the cells and the growth factors. The source was proportional to the cell and growth factor concentrations.

2.2 *Parametric sensitivity analysis*

2.2.1 *Reference computational model*

The implant described in Figure 2(a) is a polymethymethacrylate (PMMA) stable canine implant that was previously evaluated *in vivo* (Vestermark et al. 2004). The distribution pattern of newly formed tissue was symmetric around the cylindrical implant. The distribution pattern of the structural fractions ϕ_s was investigated with four transverse histological slices as shown in Figure 2(b). The average result is shown in Figure 3. As shown in Figure 2, the region of interest was defined by three parameters: the implant radius r_i, the drill-hole radius r_d and the host bone radius r_b.

The set of continuous governing Equations (1) was solved using a spatio-temporal finite difference scheme with a meshing of 0.02 mm in the radial direction *r*. The healing process was computed up to 8 weeks post-operatively according to *in vivo* experiments. All fluxes were zero at the implant surface (at radius r_i), and at the boundary of the zone of interest (radius r_b). Input data for this reference model are shown in Table 1. Geometric dimensions were based on the canine implant model and biochemical factors were estimated from literature values (Lauffenburger et al. 1983; Puleo et al. 1991; Søballe et al. 1992; Linkhart et al. 1996; Maheshwari and Lauffenburger 1998; Dee et al. 1999; Conover 2000; Roberts 2000; Bailón-Plaza and Van der Meulen 2001; Cowin 2001).

As indicated in Figure 3, the distribution pattern of the structural fraction into the tissue surrounding the implant was determined using three parameters. Parameter ϕ_{si} described the amount of mineralised tissue at the implant surface and ϕ_{sm} was the average value in the peri-implant gap post-operatively. The heterogeneity index $\Delta\phi_s$ was the difference between the minimal and maximal structural fractions in newly formed tissue.

2.2.2 *Numerical experimentation*

The robustness of the predictive model was dependent upon several mechanobiological factors. We focused on the structural fraction distribution and we implemented a statistical experimental design (Box et al. 2005) involving four variables represented at two levels, high and low, denoted by (+) and (−), respectively. The clinical aspects were represented by varying the initial growth factor concentration C_{g0} and the drill-hole radius r_d. Among the biological factors, we selected the chemotactic coefficient χ_o and the haptotactic coefficient h_o which were critical because they related to cell active migrations. To calculate sensitivities, the initial conditions of distribution were always the same constant. Other initial conditions (diffusion and concentration) related to the cell population, and the phase of growth factors were kept unchanged for all computations.

First, the output measures ϕ_{sm}, ϕ_{si} and $\Delta\phi_s$ were computed using the initial value of four variables and the response of the numerical model was noted $\bar{u}$. High levels (+) and low levels (−) were used to successively compute the new responses u noted. Second, the discrepancies between responses u and $\bar{u}$ were linearised using a

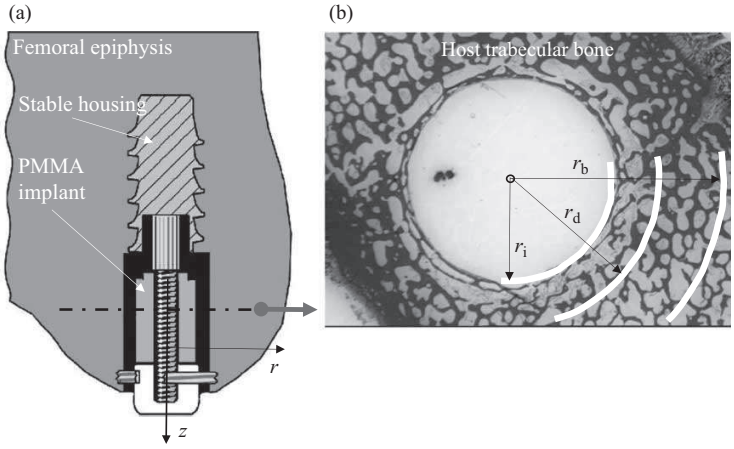

Figure 2. Canine experimental device. (a) *In vivo* implantation: the stable PMMA implant was fixed into the femoral epiphysis. (b) Histological slice showing the distribution pattern of structural fraction (Vestermark et al. 2004). In digitised histological slices, the summation of *structural fraction pixels* in successive concentric zones was divided by the pixel overall summation of the zone of interest to derive the radial distribution of structural fraction. Mean value was established on a base of four slices. r_i, implant radius; r_d, drill-hole radius; r_b, host bone radius.

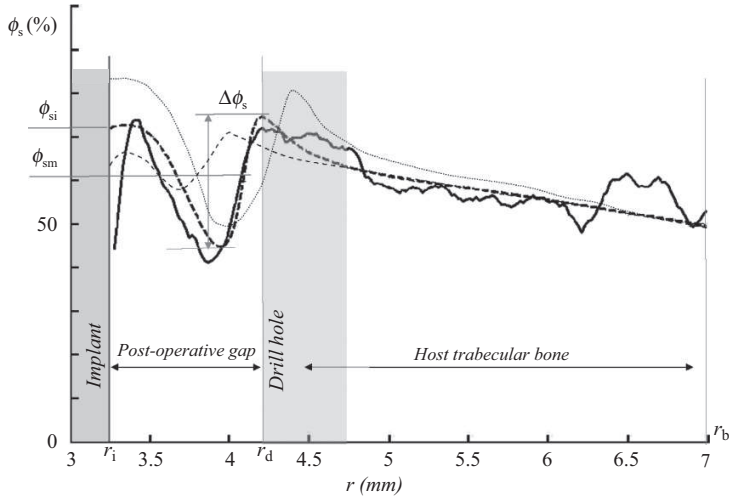

Figure 3. Distribution pattern of structural fraction ϕ_s in the periprosthetic tissue 8 weeks post-operatively. (—) Experimental results (Vestermark et al. 2004), (- - -) predictive results (Ambard and Swider 2006), (. . . .) predictive results with high level of r_d, h_0, χ_0 and C_0, (– · –) predictive results with low level of r_d, h_0, χ_0 and C_0. ϕ_{sm} was the mean value of structural fraction formed into the post-operative gap, ϕ_{si} was the structural fraction formed at the implant surface and $\Delta\phi_s$ was the heterogeneity index of the structural fraction. Radius r (mm) was measured between the implant and the host trabecular bone in the radial direction and y-axis represents the magnitude of ϕ_s. r_i, implant radius; r_d, drill-hole radius; r_b, host bone radius.

polynomial interpolation in the form of Equation (2). Coefficients a_0–a_3 described the order 1 direct effects of parameters variations on the output measures, whereas coefficients a_4–a_8 expressed the order 2 combined effects.

$$u - \bar{u} = a_0 r_d + a_1 C_g + a_2 \chi_o + a_3 h_o + a_4 r_d C_g + a_5 r_d \chi_o + a_6 r_d h_o + a_7 C_g \chi_o + a_8 C_g h_o + a_9 \chi_o h_o. \quad (2)$$

The statistical significance of a_i was established using a 95% confidence interval from a bilateral Student test as expressed by Equation (3). In this equation, p is the number of coefficients $a_i + 1$ (= 11) and s is the variance of a_i. Parameter n represents the number of calculations equal to 2^4 because the procedure involved four parameters with two levels each. The coefficient 4.03 was obtained from the Student table (Box et al. 2005).

$$\mathrm{CI}_{0.95} = \left[a_i - 4.03\sqrt{s^2/(n-p)};\ \ a_i + 4.03\sqrt{s^2/(n-p)}\right] \quad \text{with } i = 0, 9. \quad (3)$$

Our experience with the experimental canine implant model allowed the establishment of a reliable range of variation of drill-hole radius r_d to ±7%. In return, the discrepancies of the biochemical parameters were unknown and poorly documented. As a basis, we used data from the literature (Lauffenburger et al. 1983; Puleo et al. 1991; Søballe et al. 1992; Linkhart et al. 1996; Maheshwari and Lauffenburger 1998; Dee et al. 1999; Conover 2000; Roberts 2000; Bailón-Plaza and Van der Meulen 2001; Cowin 2001; Geris et al. 2008) to define plausible ranges of ±55% for h_0, ± 75% for χ_0 and ±25% for C_{g0}.

Table 1. Model data of the stable PMMA canine implant (Lauffenburger et al. 1983; Puleo et al. 1991; Søballe et al. 1992; Linkhart et al. 1996; Maheshwari and Lauffenburger 1998; Dee et al. 1999; Conover 2000; Roberts 2000; Bailón-Plaza and Van der Meulen 2001; Cowin 2001).

	Constant data		Stat. exp. design
Geometry	$r_i = 3.25$ mm	$r_b = 7$ mm	$r_d = 4.1 \pm 7\%$ mm
Cells (osteoblasts)	$\alpha_o = 1.9 \times 10^{-10}$ m^3/cell s	$D_o = 2.5 \times 10^{-7}$ mm^2/s	$h_o = 0.51 \pm 55\%$ mm^5/s kg
	$n_o = 10^3$ cell/mm^3	$\alpha_s = 2 \times 10^{-9}$ mm^6/cell s ng	$\chi_o = 4 \times 10^{-5} \pm 75\%$ mm^5/s ng
	$C_o = 10^3$ cell/mm^3	$\rho_s = 2.57 \times 10^{-6}$ kg/mm^3	
Growth factors	$D_g = 4.8 \times 10^{-6}$ mm^2/s		$C_{g0} = 0.2 \pm 25\%$ ng/mm^3

Note: The statistical experimental design involved four variables: r_d, h_o, χ_o and C_g represented at two levels, high and low, denoted by (+) and (−), respectively.

3. Results

The experimental and theoretical results of the reference model (Ambard and Swider 2006) are shown in Figure 3. The structural fraction increased from 50% in the host bone to 70% at the drill hole. The averaged fraction ϕ_{sm} was 60% and the heterogeneity index $\Delta\phi_s$ was 30%. At the implant surface, the structural fraction ϕ_{si} was 70%.

Bar diagrams in Figure 4 represented coefficients a_i and associated confidence intervals for ϕ_{si} (Figure 4(a)), ϕ_{sm} (Figure 4(b)) and $\Delta\phi_s$ (Figure 4(c)). The polynomial Equation (2) was reduced to Equation (4) using the significant coefficients a_i. The algebraic sign of a_i demonstrated whether the effect was favourable on the output measure u (+); (−) signified a negative effect.

$$\begin{aligned}
\phi_{si} - \bar{\phi}_{si} &= 10.9 \times r_d + 11.5 \times C_g + 11.9 \times \chi_o, \quad \text{(a)} \\
\phi_{sm} - \bar{\phi}_{sm} &= 7.8 \times r_d + 8 \times C_g + 6.5 \times \chi_o - 3.1 \\
&\quad \times h_o + 1.2 \times r_d C_g + 1.8 \times C_g \chi_o, \text{(b)} \\
\Delta\phi_s - \Delta\bar{\phi}_s &= 10.4 \times h_o. \quad \text{(c)}
\end{aligned} \tag{4}$$

Equation (4a) and Figure 4(a) show that three parameters had a predominant effect on the structural fraction ϕ_{si} at the implant surface: the drill hole, the growth factor concentration and the chemotactic migration. As expressed by Equation (4b) and plotted in Figure 4(b), the mean structural fraction ϕ_{sm} in the post-operative gap was influenced by the same parameters but it was noticed that haptotactic migration showed a negative contribution. At this point, two combined effects involving growth factor, drill hole and chemotactic migration were observed. Equation (4c) and Figure 4(c) show the predominant role of haptotactic migration on the heterogeneity index. We also observed that larger confidence intervals were obtained for the structural fraction at the implant surface ϕ_{si}.

4. Discussion

The theoretical model based on reactive transport in porous media showed a good ability to represent the tissue pattern with a set of conditions of a stable PMMA implant (Vestermark et al. 2004). The fluid phase strongly interacted with the cell and growth factor phases. The fundamental mechanisms were modelled using diffusive properties combined to convection and source terms in which the role of active migrations was significant.

The initial conditions of the healing process were critical and it was challenging to mimic *in vivo* conditions because of variability of the experimental model and surgical technique. We assumed that the osteoblast concentration was initially the same for the post-operative gap and into the underlying host bone. To model the initial bleeding due to surgery, we assumed that growth factors were concentrated into the post-operative gap and their concentration into the host bone was comparatively negligible.

We found that the initial growth factors concentration was always favourable to the structural fraction synthesis into the post-operative gap and at the implant surface. The influence on the heterogeneity was not significant. Among anabolic growth factors, TGF-β1 is the major regulator of bone formation. It involves a mitogenic action on osteoblasts and it shows the ability to stimulate matrix formation via autocrine, paracrine and endocrine modes (Conover 2000; Roberts 2000). Substrate properties also modify the amount of growth factors produced by osteoblasts (Puleo et al. 1991; Ramamurti et al. 1997; Overgaard 2000; Pessková et al. 2007; Popat et al. 2007; Puthumanapully et al. 2008). Owing to a lack of reliable data in the literature, we generally overestimated the range of variation of the initial growth factor concentration. The resulting theoretical model generally showed the same tendencies for positive bone growth as those observed clinically.

We fixed the drill-hole size and its variation from our experience with the experimental canine implant. The model showed that the presence of an initial gap between the implant surface and the host bone allowed apposition of mineralised tissue with no significant influence on the heterogeneity. This result was obtained with initial growth factor concentrations and initial osteoblast concentrations, which were constant independent from the gap size. Therefore the amount of growth factors and cells increased with the drill-hole size. This constituted good conditions for the osteoblastic phase to find an available volume for proliferation and bone apposition.

Stable conditions with a non-critical gap were the initial conditions of the investigated implant. These conditions checked *in vivo* were taken into account in the theoretical model. Clinically, it is known that the larger the gap is, the more likely the implant is not well secured. Micromotion is unfavourable to the long-term survival of the implant fixation. Another issue is that critical gaps might delay the healing process to the detriment of primary stability. The process does not occur via an intramembranous ossification anymore but via an endochondral process, and our model finds a limitation. The surgical technique might modify the initial response of the host bone. Alteration of microvessels could modify nutrient sources and influence subsequent angiogenesis. Combination with mechanical stimuli needs to be investigated in further studies.

Material properties and surface modification of implants affect cell adhesion and proliferation, and growth factor production (Wakefield et al. 1990; Kieswetter et al. 1996; Anderson 2001; Kilpadi et al. 2001; Colnot et al. 2007; Popat et al. 2007; Rausch-Fan et al. 2008). It is

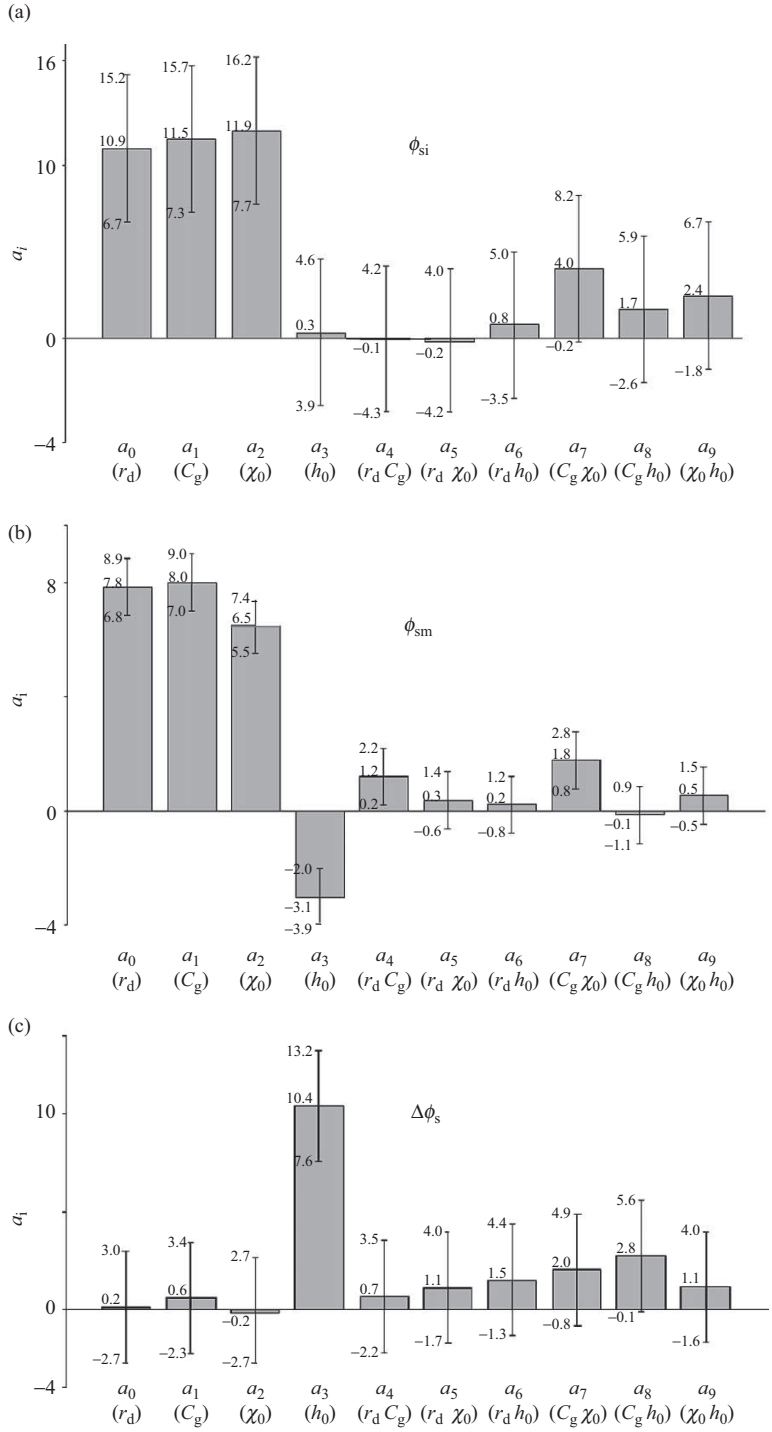

Figure 4. Sensitivity analysis of structural fraction in the periprosthetic tissue to four variables: the drill-hole radius r_d, the growth factor concentration C_g, the chemotactic coefficient χ_o and the haptotactic coefficient h_o. Bars represent the magnitude of polynomial coefficients a_i of Equation (2) and their confidence intervals. (a) Structural fraction ϕ_{si} at the implant surface (Equation (4a)), (b) mean structural fraction ϕ_{sm} (Equation (4b)), (c) heterogeneity index $\Delta\phi_s$ (Equation (4c)).

observed that sensitivity to surface topology is significant (Neidlinger-Wilke et al. 1994; Fermor et al. 1998; Pessková et al. 2007) and generally, osteoblastic proliferation decreases when surface roughness increases (Martin et al. 1995; Mustafa et al. 2001; Rosa and Beloti 2003).

We previously proposed a preliminary model of interactions with bioactive surfaces (Guérin et al. 2009). Osteoblast adhesion properties and growth factor source were locally updated to model biochemical interactions of implant with its environment. We found that the decrease in cell diffusion significantly improved the amount of mineralised tissue on the implant surface. However, the model also confirmed that implant bioactive properties should play a limited role to reduce heterogeneity of newly formed tissue.

The parameters associated with active migrations are poorly documented in the literature, especially in an *in vivo* setting, yet their roles are of prime importance in the healing process. Our model considered cells as a continuous phase and it allowed active migrations to be involved in convective terms and source terms. To determine the tendencies, we created ranges for biochemical factors based on literature review. We varied the haptotactic coefficient by $\pm 75\%$ and varied the chemotactic coefficient by $\pm 25\%$.

We observed that the haptotactic coefficient reduced apposition of structural fraction in the newly formed tissue, and its influence on the heterogeneity index was predominant. To potentially explain this result, we observed that the greater porosity gradient was initially located at the drill hole. At the drill-hole edge, the cells migrating from the host bone towards the implant could find favourable adhesion sites to proliferate and synthesise mineral matrix. The cells initially present in the post-operative gap could be attracted towards the drill hole also because of adhesion sites. Finally, the decrease in local porosity because of mineralised tissue apposition limited the access to new cells and favoured heterogeneity of the healing.

We found that the chemotactic migration increased the structural fraction between the drill hole and the implant surface, whereas no significant influence on the heterogeneity was detected. We assumed as an initial condition that growth factors were only concentrated into the initial gap. Growth factor concentration was significantly greater in the gap compared to surrounding host bone because of initial bleeding due to surgery. It was assumed that there were initially no growth factors in the host bone and this induced a gradient between these two zones. Even if they diffused and were transported by fluid flux, the algebraic sign of their concentration gradient was unchanged during the healing process and it was always oriented from the host bone towards the implant. This gradient attracted cells located in the host bone whereas those initially present in the post-operative gap were not recruited.

Finally, the combination of haptotactic flux and chemotactic flux strongly influenced the distribution pattern of structural fraction apposition varying from the implant surface towards the host bone.

In conclusion, we could note that the theoretical results presented noticeable similarities with the empirical results observed clinically (Søballe et al. 1992; Vestermark et al. 2004; Franchi et al. 2005). A sensitivity analysis helped to objectively identify the relative dependence of implant healing on several mechanobiological parameters.

To implement a statistical experimental design convenient in interpretation, we initially limited the number of variable parameters to four. However, we plan to add three variables to raise the clinical relevance. The osteoblast initial concentration and the initial porosity of the host bone could be involved to evaluate the role of bone pathologies such as osteoporosis on implant fixation. We also plan to study surgical technique by modifying the drill-hole profile irregularities and size.

Our study also showed that the investigation of growth factor mode of production could be of particular interest. A preliminary model of local interactions with the implant bioactive surface of implant has been proposed (Guérin et al. 2009) and this will be completed by relevant source terms involving the post-operative neovascularisation.

Acknowledgements

The French Minister of Education and Research is acknowledged for its assistance. Related experimental studies were conducted with the support of NIH AR4205, Institute of Pathology at Aarhus University Hospital, Orthopaedic Research and Education Foundation, Danish Research Foundation for Health, Master of a guild, butcher Peter Ryholts Foundation and the Danish Rheumatism Association, and Anna and Jakob Jakobsens Foundation. Biomet donated the PMMA implants.

References

Albrektsson T, Brånemark PI, Hansson HA, Kasemo B, Larsson K, Lundström I, McQueen DH, Skalak R. 1983. The interface zone of inorganic implants *in vivo*: titanium implants in bone. Ann Biom Eng. 11:1–27.

Ambard D, Pedrono A, Swider P. 2005. A predictive numerical model of the periprosthetic tissue formation surrounding a stable implant. Paper presented at: 50th Annual Meeting of Orthopaedic Research Society; USA.

Ambard D, Swider P. 2006. A predictive mechano-biological model of the bone-implant healing. Eur J Mech/A Sol. 25:927–937.

Anderson JM. 2001. Biological responses to materials. Ann Rev Mat Res. 31:81–110.

Bailón-Plaza A, Van der Meulen MC. 2001. A mathematical framework to study the effects of growth factor influences on fracture healing. J Theor Biol. 212:191–209.

Box GEP, Hunter WG, Hunter JS. 2005. Statistics for experimenters: design, innovation, and discovery. 2nd ed. New York: Wiley.

Checa S, Prendergast PJ. 2009. A mechanobiological model for tissue differentiation that includes angiogenesis: a lattice-based modeling approach. Ann Biom Eng. 37:129–145.

Colnot C, Romero DM, Huang S, Rahman J, Currey JA, Nancy A, Brunski JB, Helms JA. 2007. Molecular analysis of healing at a bone-implant interface. J Dent Res. 86:862–867.

Conover CA. 2000. Insulin-like growth factors and the skeleton. In: Canalis E, editor. Skeletal growth factors. New York: Lippincott Williams & Wilkins. p. 101–116.

Cowin SC. 2001. Bone mechanics handbook. Boca Raton, FL: CRC Press.
Dee KC, Anderson TT, Bizios R. 1999. Osteoblast population migration characteristics on substrates modified with immobilized adhesive peptides. Biomaterials. 20(3): 221–227.
Fall CP, Marland ES, Wagner JM, Tyson JJ. 2002. Computational cell biology. Interdisciplinary applied mathematics. New York: Springer-Verlag.
Fermor B, Gundle R, Evans M, Emerton M, Pocock A, Murray D. 1998. Primary human osteoblast proliferation and prostaglandin E_2 release in response to mechanical strain *in vitro*. Bone. 22:637–643.
Franchi M, Fini M, Giavaresi G, Ottani V. 2005. Peri-implant osteogenesis in health and osteoporosis. Micron. 36:630–644.
Friedl P, Zanker KS, Brocker EB. 1998. Cell migration strategies in 3-D extracellular matrix: differences in morphology, cell matrix interactions, and integrin function. Microsc Res Tech. 43(5):369–378.
Geris L, Gerisch A, Sloten JV, Weiner R, Oosterwyck H. 2008. Angiogenesis in bone fracture healing: a bioregulatory model. J Theor Biol. 251(1):137–158.
Guérin G, Ambard D, Swider P. 2009. Cells, growth factors and bioactive surface properties in a mechanobiological model of implant healing. J Biomech. 42(15):2555–2561.
Hahn M, Vogel M, Eckstein F, Pompesius-Kempa M, Delling G. 1998. Bone structure changes in hip joint endoprosthesis implantation over the course of many years. A quantitative study. Chirurg. 59(11):782–787.
Kibbin MB. 1998. The biology of fracture healing in long bones. J Bone Joint Surg A. 79:1938–1941.
Kieswetter K, Schwartz Z, Hummert TW, Cochran DL, Simpson J, Dean DD, Boyan BD. 1996. Surface roughness modulates the local production of growth factors and cytokines by osteoblast-like MG-63 cells. J Biomed Mater Res. 32:55–63.
Kilpadi KL, Chang PL, Bellis SL. 2001. Hydroxylapatite binds more serum proteins, purified integrins, and osteoblast precursor cells than titanium or steel. J Biomed Mater Res. 57:258–267.
Lauffenburger D, Rothman C, Zigmond SH. 1983. Measurement of leukocyte and chemotaxis parameters with a linear under-agarose migration assay. J Immunol. 131:940–947.
Linkhart TA, Mohan S, Baylink DJ. 1996. Growth factors for bone growth and repair: IGF, TGF beta and BMP. Bone. 19(1 Suppl):1S–12S. Review.
Maheshwari G, Lauffenburger DA. 1998. Deconstructing (and reconstructing) cell migration. Microsc Res Tech. 43(5):358–368.
Martin JY, Schwartz Z, Hummert TW, Schraub DM, Simpson J, Lankford J, Jr, Dean DD, Cochran DL, Boyan BD. 1995. Effect of titanium surface roughness on proliferation, differentiation, and protein synthesis of human osteoblast-like cells (MG63). J Biomed Mater Res. 29:389–401.
Meinel L, Zoidis E, Zapf J, Hassa P, Hottiger MO, Auer JA, Schneider R Gander B, Luginbuehl V, Bettschart-Wolfisberger R, et al. 2003. Localized insulin-like growth factors I delivery to enhance new bone formation. Bone. 33(4):660–672.
Morshed S, Bozic KJ, Ries MD, Malchau H, Colford JM, Jr. 2007. Comparison of cemented and uncemented fixation in total hip replacement: a meta-analysis. Acta Orthop. 78(3):315–326.
Mustafa K, Wennerberg A, Wroblewski J, Hultenby K, Lopez BS, Arvidson K. 2001. Determining optimal surface roughness of TiO(2) blasted titanium implant material for attachment, proliferation and differentiation of cells derived from human mandibular alveolar bone. Clin Oral Implants Res. 12:515–525.
Neidlinger-Wilke C, Wilke HJ, Claes L. 1994. Cyclic stretching of human osteoblasts affects proliferation and metabolism: a new experimental method and its application. J Orthop Res. 12:70–78.
Overgaard S. 2000. Calcium phosphate coatings for fixation of bone implants. Acta Orthop Scand. 71(Suppl 297):1–74.
Pessková V, Kubies D, Hulejová H, Himmlová L. 2007. The influence of implant surface properties on cell adhesion and proliferation. J Mater Sci Mater Med. 18:465–473.
Popat KC, Leoni L, Grimes CA, Desai TA. 2007. Influence of engineered titania nanotubular surfaces on bone cells. Biomaterials. 28:3188–3197.
Puleo DA, Holleran LA, Doremus RH, Bizios R. 1991. Osteoblast responses to orthopedic implant materials *in vitro*. J Biomed Mater Res. 25(6):711–723.
Puthumanapully P, New A, Browne M. 2008. Do multi-layer beads on porous coated implants influence bone ingrowth? A finite element study. J Biomech. 41:S290.
Ramamurti BS, Orr TE, Bragdon CR, Lowenstein JD, Jasty M, Harris WH. 1997. Factors influencing stability at the interface between a porous surface and cancellous bone: a finite element analysis of a canine *in vivo* micromotion experiment. J Biomed Mater Res. 36(2):274–280.
Rausch-Fan X, Qu Z, Wieland M, Matejka M, Schedle A. 2008. Differentiation and cytokine synthesis of human alveolar osteoblasts compared to osteoblast-like cells (MG63) in response to titanium surfaces. Dent Mater. 24(1):102–110.
Roberts AB. 2000. Transforming growth factor-β? In: Canalis E, editor. Skeletal growth factors. Philadelphia, PA: Lippincott Williams & Wilkins. p. 221–232.
Rosa AL, Beloti MM. 2003. Rat bone marrow cell response to titanium and titanium alloy with different surface roughness. Clin Oral Implants Res. 14:43–48.
Schwarz F, Herten M, Sager M, Wieland M, Dard M, Becker J. 2007. Histological and immunohistochemical analysis of initial and early osseous integration at chemically modified and conventional SLA titanium implants: preliminary results of a pilot study in dogs. Clin Oral Implants Res. 18:481–488.
Søballe K, Hansen ES, B-Rasmussen H, Jorgensen PH, Bunger C. 1992. Tissue ingrowth into titanium and hydroxyapatite-coated implants during stable and unstable mechanical conditions. J Orthop Res. 10(2):285–299.
Vestermark MT, Bechtold JE, Swider P, Søballe K. 2004. Mechanical interface conditions affect morphology and cellular activity of sclerotic bone rims forming around experimental loaded implants. J Orthop Res. 22(3):647–652.
Wakefield LM, Winokur TS, Hollands RS, Christopherson K, Levinson AD, Sporn AB. 1990. Recombinant latent transforming growth factor β1 has a longer plasma half-life in rats than active transforming growth factor β1, and a different tissue distribution. J Clin Invest. 86:1976–1984.
Wang JY, Wicklund BH, Gustilo RB, Tsukayama DT. 1997. Prosthetic metals interfere with the functions of human osteoblast cells *in vitro*. Clin Orthop Rel Res. 339:216–226.

Appendix 1

The local variation L, the convective term C, the diffusive term D and the source term Ω of governing Equation (1) were expressed by Equations (A1)–(A4). Output measure u was the extracellular fluid flux q_f, the osteoblastic concentration C_o, the growth factor concentration C_g and the structural fraction ϕ_s.

u	L	C	D	Ω	
q_f	0	1	0	$\frac{\partial \phi_f}{\partial t}$	(A1)
C_o	ϕ_f	$\phi_f \chi_o \frac{\partial C_g}{\partial x} - \frac{\partial \phi_f}{\partial x}(D_o + \rho h_o \phi_f)$	$D_o \phi_f$	$C_o\left[\frac{-\partial \phi_f}{\partial t} + h_o \rho\left[\phi_f \frac{\partial^2 \phi_f}{\partial x^2} + \left(\frac{\partial \phi_f}{\partial x}\right)^2\right]\right.$ $- \chi_o\left[\phi_f \frac{\partial^2 C_g}{\partial x^2} + \frac{\partial C_g}{\partial x}\frac{\partial \phi_f}{\partial x}\right]$ $\left. + \alpha_o \phi_f (n_o - \phi_f C_o)\right]$	(A2)
C_g	ϕ_f	$-\left(q_f + D_g \frac{\partial \phi_f}{\partial x}\right)$	$D_g \phi_f$	0	(A3)
ϕ_s	1	0	0	$\alpha_s C_g C_o \phi_f^2$	(A4)